TISSUE ENGINEERING

Computational modeling guides tissue-engineered heart valve design for long-term in vivo performance in a translational sheep model

Maximilian Y. Emmert,[1,2,3]* Boris A. Schmitt,[4,5]* Sandra Loerakker,[6,7]* Bart Sanders,[6,7]* Hendrik Spriestersbach,[4,5] Emanuela S. Fioretta,[1] Leon Bruder,[4,5] Kerstin Brakmann,[4,5] Sarah E. Motta,[1] Valentina Lintas,[1] Petra E. Dijkman,[1] Laura Frese,[1] Felix Berger,[4,5]† Frank P. T. Baaijens,[6,7]† Simon P. Hoerstrup[1,3]†‡

Valvular heart disease is a major cause of morbidity and mortality worldwide. Current heart valve prostheses have considerable clinical limitations due to their artificial, nonliving nature without regenerative capacity. To overcome these limitations, heart valve tissue engineering (TE) aiming to develop living, native-like heart valves with self-repair, remodeling, and regeneration capacity has been suggested as next-generation technology. A major roadblock to clinically relevant, safe, and robust TE solutions has been the high complexity and variability inherent to bioengineering approaches that rely on cell-driven tissue remodeling. For heart valve TE, this has limited long-term performance in vivo because of uncontrolled tissue remodeling phenomena, such as valve leaflet shortening, which often translates into valve failure regardless of the bioengineering methodology used to develop the implant. We tested the hypothesis that integration of a computationally inspired heart valve design into our TE methodologies could guide tissue remodeling toward long-term functionality in tissue-engineered heart valves (TEHVs). In a clinically and regulatory relevant sheep model, TEHVs implanted as pulmonary valve replacements using minimally invasive techniques were monitored for 1 year via multimodal in vivo imaging and comprehensive tissue remodeling assessments. TEHVs exhibited good preserved long-term in vivo performance and remodeling comparable to native heart valves, as predicted by and consistent with computational modeling. TEHV failure could be predicted for nonphysiological pressure loading. Beyond previous studies, this work suggests the relevance of an integrated in silico, in vitro, and in vivo bioengineering approach as a basis for the safe and efficient clinical translation of TEHVs.

INTRODUCTION

Current bioengineering approaches aiming to create living organ and tissue replacements with "native-analogous" self-repair, regeneration, and growth capacity have gained considerable scientific attention and are expected to enable "game-changing" next-generation therapies. However, the efficient translation from experimental proof of concept to routine clinical use has been slower than expected because of multifaceted logistical, technical, and regulatory challenges (*1*). A major roadblock to clinically safe and robust tissue engineering (TE) solutions is the high complexity and variability inherent to bioengineering technologies that rely on cell-driven remodeling, regeneration, and growth. In the light of the lessons learned from more than 20 years in various heart valve TE research projects, here, we tested whether an analytical design, inspired by computational modeling, can consistently guide tissue remodeling and ensure long-term functionality in tissue-engineered heart valves (TEHVs).

Valvular heart disease is associated with a high morbidity and mortality worldwide (*2*). Despite well-established surgical and transcatheter-based therapeutic approaches to either repair or replace diseased heart valves, the currently available, essentially nonregenerative prostheses have major limitations such as thromboembolic and bleeding complications and limited durability due to progressive dysfunctional degeneration (*3*, *4*). In particular, none of these prostheses has the unique properties of native heart valves to continuously adapt to changes in the hemodynamic environment (*5*). Consequently, many of the patients implanted with these inert heart valves are exposed to a lifelong risk for valve prosthesis–related morbidity and mortality. As a particularly vulnerable patient population, children with congenital heart malformation often require multiple reoperations due to the lack of growth inherent to current prosthetic materials, which is associated with an exponentially increased risk for surgical complications (*6*, *7*).

The concept of heart valve TE that creates heart valves with self-repair, remodeling, and growth capacity represents a promising alternative to contemporary prostheses used clinically. With the introduction of the TE concept more than 20 years ago (*8*), numerous different heart valve TE approaches have been developed and tested demonstrating principal feasibility in preclinical large-animal models (*9*–*22*). TE concepts were further merged with the latest minimally invasive implantation technologies, and simplifications of the multistep in vitro heart valve TE approaches toward optimized and more clinically relevant "off-the-shelf" strategies were established. Accordingly, in situ TE concepts relying on the recipient's body to regenerate the implant in vivo represent the most advanced and clinically relevant methodology. In particular, tissue-engineered extracellular matrices (ECMs) depleted of cells have proven to be a valid off-the-shelf alternative to the initially described in vitro TE approaches in several

[1]Institute for Regenerative Medicine, University of Zurich, Zurich, Switzerland. [2]University Heart Center Zurich, University Hospital Zurich, Zurich, Switzerland. [3]Wyss Translational Center Zurich, University of Zurich and ETH Zurich, Zurich, Switzerland. [4]German Heart Center Berlin and Charité—Universitätsmedizin Berlin, Department of Congenital Heart Disease, Berlin, Germany. [5]DZHK (German Centre for Cardiovascular Research), partner site Berlin, Berlin, Germany. [6]Department of Biomedical Engineering, Eindhoven University of Technology, Eindhoven, Netherlands. [7]Institute for Complex Molecular Systems, Eindhoven University of Technology, Eindhoven, Netherlands.
*These authors contributed equally to this work as first authors.
†These authors contributed equally to this work as last authors.
‡Corresponding author. Email: simon.hoerstrup@irem.uzh.ch

preclinical investigations (*11*, *12*, *15*, *18*, *22*). Furthermore, the principal feasibility of implanting biodegradable polymeric scaffolds in a preclinical animal model, which are transformed into cell-repopulated valves in vivo, has been recently demonstrated (*10*).

However, the long-term proof of such concepts is still pending. The functionality of most TEHVs is gradually lost within a few months due to adverse tissue remodeling, which translates into the development of leaflet retraction and valvular incompetence almost universally and independently of the bioengineering methodology used (*11*, *12*, *15*, *17*, *18*, *20*–*22*). Understanding and guiding the mechanisms of functionally adaptive and potentially maladaptive remodeling are therefore of central importance for safe and efficient clinical translation.

Leaflet retraction has been mainly described as a consequence of tissue contraction by α–smooth muscle actin (αSMA)–positive cells and leaflet-wall fusion phenomena resulting from maladaptive remodeling. Because the degree of αSMA expression and cardiovascular tissue remodeling in general are known to strongly interrelate with mechanical cues (*23*–*27*), we hypothesize that improving the mechanical behavior of TEHVs is key to ensuring physiological remodeling and long-term functionality. Computational modeling of valve mechanics and corresponding tissue remodeling provides a powerful approach to predict the consequences of changes in valve design on the overall outcome. However, despite the widespread use of modeling to optimize the performance of traditional valve replacements (*28*, *29*), it has been used only rarely to improve TEHV functionality (*30*, *31*).

In a recent study (*32*), we suggested that previous "simplified" valve designs are major driving factors for leaflet retraction. Computational modeling indicated that such designs lead to nonphysiological tissue compression in the radial direction during diastole, presumably acting in synergy with αSMA cell contractility to induce leaflet retraction. Because our computational predictions indicated that a more physiological valve geometry in combination with a relatively large coaptation area would considerably increase the radial stretch of TEHVs and hence potentially reduce the development of retraction (*32*), we designed geometrical constraints to incorporate this geometry into our multistep in vitro heart valve culture procedure (*33*).

Here, we conducted a large-animal study in a clinically and regulatory (U.S. Food and Drug Administration and European Medicines Agency) relevant sheep model over 1 year to test the hypothesis that a computationally inspired valve design leads to superior remodeling and functionality compared to our previous works (*15*, *22*), based on otherwise identical in vitro engineering technology. We use computational modeling to predict the in vivo remodeling process and to understand potential differences in outcomes. After an outline on valve manufacturing and transcatheter implantation as pulmonary heart valve replacements into adult sheep, we provide the longitudinal assessment of long-term valve functionality using state-of-the-art imaging methods. Furthermore, we focus on a comprehensive analysis of the explanted valves to demonstrate the remodeling potential of TEHV based on computational modeling–inspired design.

RESULTS

Analytical design, TEHV production, and in vitro functionality

TEHVs with computationally inspired geometry ($n = 15$; valves A to O, table S1), aiming at increasing the radial stretch of the leaflets during diastole, were cultured as described previously to obtain a physiologically relevant design with belly curvature (fig. S1) (*32*, *33*). In brief, a relatively large coaptation area was included in the design to address potential retraction phenomena in this region as documented in our previous preclinical studies (*15*, *22*) and predicted in a recent computational study (*34*). For all valves, ECM was deposited by vascular-derived cells (myofibroblasts), and tissue was properly formed throughout the valve during the in vitro generation process. After decellularization (*35*), the geometry (belly curvature and coaptation length) was maintained using geometrical constraints (Fig. 1, A and B). Decellularized TEHVs showed successfully preserved ECM with no evidence of cellular remnants (fig. S2). Before implantation, adequate in vitro valve functionality was demonstrated in a pulse duplicator system by the presence of symmetrical opening and closing behavior and good leaflet motility (movie S1), with no signs of stenosis or relevant regurgitation (Fig. 1C). The average regurgitation fraction before implantation was 9.29 ± 2.90%, of which the majority (8.17 ± 3.11%) was resulting from the natural closing volume of the valve (table S1). Computational simulations based on material parameters derived from biaxial tensile tests of valves ($n = 4$) before implantation ($R^2 > 0.99$) demonstrated that TEHVs would mainly stretch in the circumferential direction during diastole, whereas radial compression was almost completely prevented (compressive strains, <2%) (Fig. 1, D and E).

Transcatheter implantation of TEHVs as pulmonary valve replacement in adult sheep

Transcatheter delivery of TEHVs as pulmonary valve replacements using a fully percutaneous trans-jugular access was successfully performed in 11 adult sheep (tables S2 and S3 and figs. S1 and S3A) with appropriate positioning in 10 of 11 animals. In these animals ($n = 10$), post-procedural angiography (fig. S3C) showed immediate TEHV function, yielding physiological results with no or only minor regurgitation (movie S2). Next, hemodynamic assessment performed 1 week after surgery revealed hemodynamics comparable to native pulmonary valves, with a low trans-valvular systolic gradient over the TEHV (4.5 ± 2.8 mmHg; table S4) and without any sign of stenosis. A cardiac computed tomography (CT) 1 week after implantation confirmed appropriate positioning of these valves (fig. S3B). No periprocedural adverse events, such as higher-grade ventricular arrhythmias, valve embolization, or bleeding, were observed. In one animal, the TEHV was implanted too distally, thereby not fully excluding the native pulmonary valve (valve G). This resulted in a suboptimal loading of the TEHV and a higher-grade (mild to moderate) insufficiency. Therefore, this TEHV was excluded from the study (see fig. S4 for further details).

Preserved long-term in vivo performance of TEHVs 1 year after implantation

Longitudinal multimodal imaging assessment of the TEHVs ($n = 10$) using intracardiac echocardiography (ICE; fig. S3D) and cardiac magnetic resonance imaging (MRI; fig. S3E) 1 week after delivery and then monthly until the study end at 1 year revealed unremarkable and preserved TEHV function in 9 of 10 animals, with values comparable to native pulmonary valves (Fig. 2).

Longitudinal ICE analysis displayed a mean insufficiency grade of only 0.20 ± 0.42 (trivial) 1 week after implantation and 1.05 ± 0.46 (mild) after 1 year (table S5), confirming good, preserved TEHV function throughout the study. As expected from the computational predictions and taken into account by the current TEHV design, the

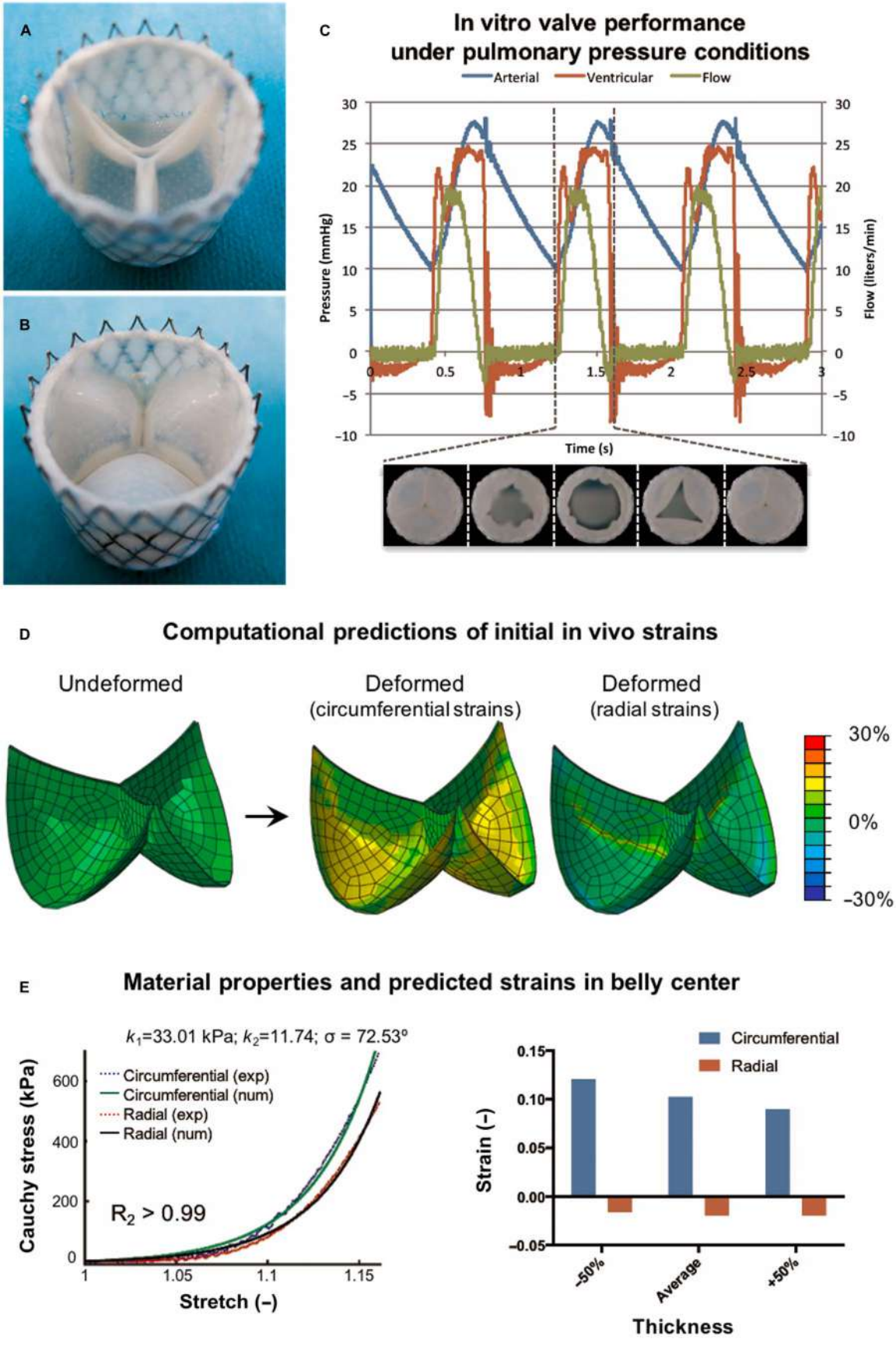

Fig. 1. TEHV manufacturing and characterization. (**A**) Macroscopic appearance of the distal and (**B**) proximal view of a representative TEHV after 4 weeks of in vitro culturing using geometrical constraints. (**C**) Representative flow and pressure curves of in vitro measurements, with representative images of the opening and closure behavior of the TEHV during the cardiac cycle. (**D**) Graphical representations of the initial in vivo circumferential (circ. strains) and radial (rad. strains) deformations as predicted by the computational model. (**E**) Average biaxial tensile test results of the control valves (n = 4) and fits of the material parameters (k_1, k_2, and σ) in the computational model (left) and predictions of the initial in vivo circumferential and radial strains in the belly center as a function leaflet thickness (right). The R^2 value (left) indicates to what extent the model can predict the experimental data (with a maximum of 1).

coaptation areas shortened from 7.0 mm (2.0 to 12.0 mm) immediately after implantation to 3.0 mm (1.0 to 5.0 mm) at 6 months after surgery ($P = 0.039$) but then remained stable until the end of the study at 12 months ($P = 1.00$) (Fig. 2, A to C). This indicates that the shortening mainly occurred in the unloaded region of the valve within the first 6 months as part of a functional remodeling response, after which an equilibrium was reached. Next, Doppler evaluation displayed a comparable maximum antegrade flow velocity (V_{max}) across the TEHV at 1 week (0.87 ± 0.33 m/s) and 1 year (1.14 ± 0.24 m/s) after implantation. Moreover, low-pressure gradients at 1 week (3.35 ± 3.17 mmHg) and after 1 year (5.41 ± 2.30 mmHg) were indicative of unobstructed systolic flow (table S5), as also confirmed by invasive trans-valvular mean pressure gradient measurements (4.5 ± 2.8 mmHg at 1 week versus 6.1 ± 8.6 mmHg at 1 year) (table S4).

In line with the ICE data, longitudinal two-dimensional quantitative cardiac MRI flow measurements in the main pulmonary artery at the distal end of the TEHV confirmed unremarkable and preserved functionality in 9 of 10 TEHVs throughout the study period, with a low mean regurgitation fraction of 9.7 ± 4.2% after 1 week and 13.9 ± 5.7% after 1 year (Fig. 2D, fig. S5, and table S6). One TEHV (valve E) showed an unremarkable performance for up to 4 months after implantation but then developed a higher-grade insufficiency (regurgitation fraction of >30% in two consecutive MRI assessments). As per protocol, this TEHV was explanted at 6 months and excluded from the main analysis (Fig. 2D and figs. S5 and S6 for further details on valve E).

Prediction of in vivo remodeling and functionality from the initial valve properties

We used computational modeling (*34*, *36*–*38*) to predict the in vivo remodeling of TEHVs in response to dynamic pressure variations, starting from the initial geometry and material properties before implantation (see the "Computational prediction of valve functionality and remodeling" section of Supplementary Materials and Methods for a detailed description). Systematic variations of leaflet thickness and cell contractility were performed to assess their role in ensuring functional remodeling. In all simulations, remodeling was predicted to induce a stable tissue architecture. As part of functional remodeling, tissue compaction (represented by compressive strains during diastole) was predicted to occur primarily in the radial direction with maximum values occurring in the coaptation area (Fig. 3A), consistent with our previous predictions (*34*). The total amount of compaction increased with leaflet thickness and cell contractility (fig. S7A). Successful valve performance (diastolic orifice area, <0.5%) was predicted for all leaflet thicknesses when cell contractility was low (Fig. 3B and fig. S7B). Because the latter assumption was valid for the current study, this predicted functionality was in line with the in vivo observations (Fig. 2 and movies S3 to S8). Increasing cell contractility in the simulations, however, corresponded to a reduction in coaptation (fig. S7B). A slightly anisotropic collagen architecture was predicted with a preferred circumferential orientation in all simulations (Fig. 3C and fig. S7C). In six of the seven explants where collagen alignment was quantified (valves H to N), the measured degree of anisotropy (fig. S8) was in the range of the simulations with low cell contractility (ratio between the maximum and minimum of the fitted collagen histogram was 1.33 to 2.40; Fig. 3C). Valve N (ratio of 3.75) fell outside of this predicted range but also exhibited a considerably higher collagen alignment compared to the other six valves.

Differences between explants due to tissue properties and/or hemodynamics

To elucidate differences in outcome, dedicated computational simulations were performed based on quantitative data of material properties and collagen alignment available upon explantation [valves G (suboptimal positioning), H, I, J, and N]. Despite the differences in leaflet thickness and material properties between the individual valves, sufficient leaflet coaptation during diastole was predicted for all cases (Fig. 4, A and B) except for valve G (considerable regurgitation due to >23% valve opening during diastole; fig. S4, A to C), in agreement with experimental findings. A direct comparison of the degree of collagen alignment in the explants and the computational model (Fig. 4C) indicated a monotonic relationship between the measured alignment in the explants and the predicted collagen alignment from the simulations [Spearman rank correlation coefficient $\rho = 1$ ($P = 0.08$)], indicating that our predictive model sufficiently captured the differences in remodeling observed in vivo.

Tissue remodeling toward a native-like composition and architecture

One year after implantation, the TEHVs presented with native-like tissue configurations composed of cellular repopulation, improved matrix composition, and reorganization of collagen fibers (indicative of functional remodeling). All TEHVs displayed thin and shiny leaflet tissue with no signs of thrombosis [$n = 9$; valves G (malpositioning) and E (early harvest at 6 months) were excluded and analyzed separately; Fig. 5, A and B]. Extensive cellular repopulation was observed in the entire valve including wall, leaflet belly, and tip regions (Fig. 5C and fig. S9). The stent interface and the TEHV wall appeared to be completely integrated into the adjacent native pulmonary artery wall. In most of the TEHVs, neosinus formation was observed, contributing to a native-like valve anatomy (fig. S10A). Quantification of the leaflet dimensions indicated that leaflet length decreased significantly ($P = 0.0028$) during the 1-year period from an initial length of 18.29 mm (17.68 to 19.22 mm) [presented as median and interquartile range (IQR)] in the nonimplanted controls to 12.80 mm (11.48 to 14.06 mm) in the explants (fig. S11, A to C) without affecting valve functionality. The decrease of leaflet length (approximately 5.5 mm in total) mainly occurred in the unloaded part of the coaptation area (>70% of total shortening), as predicted by the computational models and confirmed by the corresponding ICE analysis (Fig. 2C and table S5). So-called belly wall fusion phenomena as seen in our previous studies (*15*, *22*) were not detected (Fig. 2, A to C, and fig. S11D). Leaflet thickness upon explantation was in the range of the thicknesses of the control valves or smaller (table S7).

Minimal polymeric scaffold remnants were observed in the leaflets, from the middle to the tip, whereas no remnants were found in the wall and hinge region in most of the valves (seven of nine) (Fig. 5, C to E). In some of the valves, small and functionally irrelevant microcalcifications (sized between 20 and 200 μm) colocalized with scaffold remnants in the leaflet, as confirmed by von Kossa staining (fig. S12). In cases where small polymer remnants were still present in the wall, plasma cells, macrophages, multinucleated giant cells, and lymphocytes (fig. S13) were localized, with neovascularization in the adjacent tissue, suggesting an ongoing remodeling process.

Analysis of tissue composition and architecture showed that elastin was detected with a heterogeneous distribution pattern primarily in the wall and hinge areas (Fig. 5E and fig. S10). In addition, all leaflets presented with a dense, homogeneous, and wavy collagen matrix

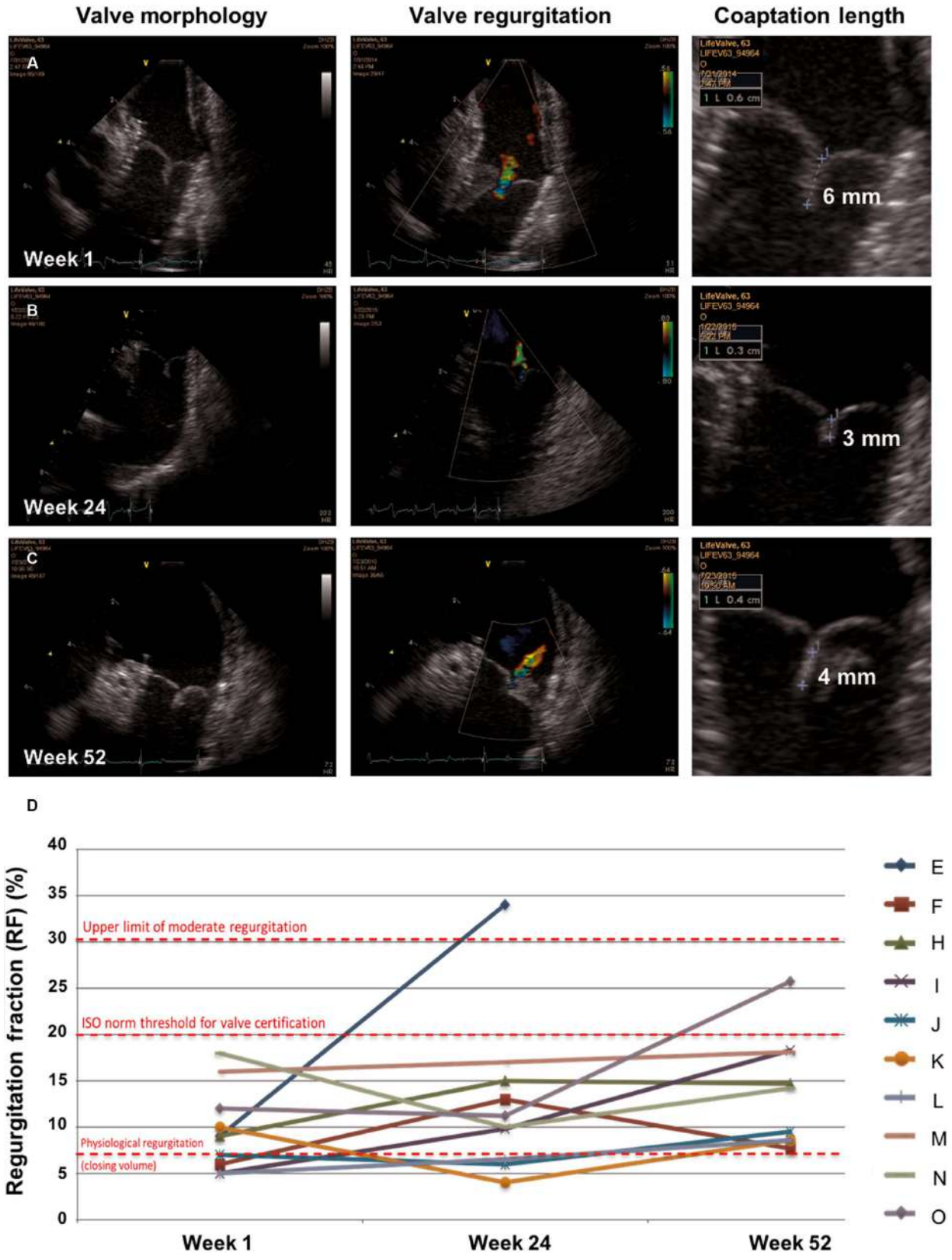

Fig. 2. Preserved long-term functionality of the TEHVs over 1-year follow-up as assessed by ICE and cardiac MRI flow measurements. (**A** to **C**) ICE evaluation on valve morphology, insufficiency grade (regurgitation), and leaflet coaptation. Exemplary imagery of valve I is shown. (**D**) Longitudinal cardiac MRI flow analysis of valve regurgitation of all valves at weeks 1, 24, and 52 after TEHV implantation (see also fig. S5).

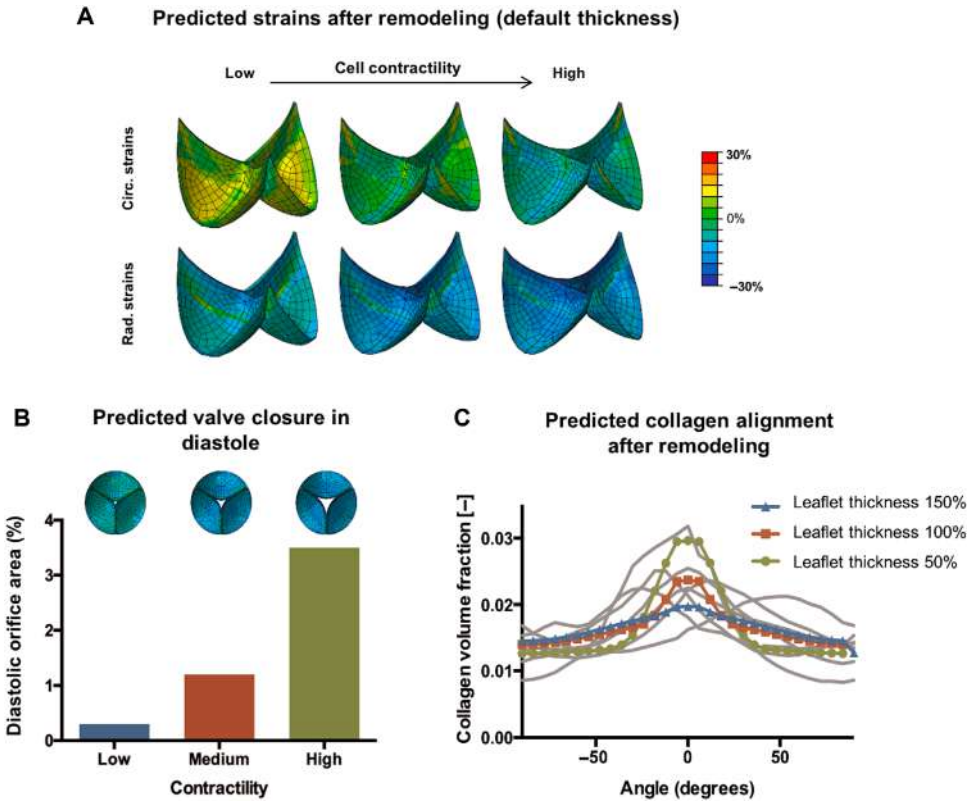

Fig. 3. Computational predictions of valve remodeling based on initial tissue properties. (**A**) Circumferential (circ.) and radial (rad.) strains in the loaded configuration upon variations in cell contractility. Results shown with the average leaflet thickness. If present, the central opening of the valve during diastole serves as an indirect measure of valvular insufficiency. (**B**) The predicted valve opening (percentage of the total orifice area and top views of the corresponding valves with average leaflet thickness during diastole) as a function of contractility. The effects of variations in leaflet thickness from the average value are reported in fig. S7B. (**C**) Predictions of collagen alignment for different leaflet thicknesses and low cell contractility (colored lines) compared to the collagen distributions measured in the explants (gray lines).

(Fig. 5, D and E, and fig. S14). Quantification of the collagen alignment by means of image analysis indicated that the degree of alignment in the circumferential direction was significantly increased (P = 0.0424) 1 year after implantation (fig. S8A).

Biochemical analyses on the ECM composition of the leaflets demonstrated that the amount of collagen [based on the amount of hydroxyproline (HYP)] increased significantly (P = 0.0028) from 37.29 μg/mg dry weight (35.80 to 41.11 μg/mg dry weight) in the nonimplanted controls to 58.98 μg/mg dry weight (54.42 to 61.31 μg/mg dry weight) (Fig. 6A), as represented by the median and IQR. However, no significant difference (P = 0.9147) in sulfated glycosaminoglycans (sGAGs) content between the nonimplanted controls [17.77 μg/mg dry weight (17.47 to 18.60 μg/mg dry weight)] and the explants [18.12 μg/mg dry weight (13.28 to 20.85 μg/mg dry weight)] was observed (Fig. 6B). DNA content significantly (P = 0.0028) increased from 0.0024 μg/mg dry weight (0.0019 to 0.0029 μg/mg dry weight) in the nonimplanted control valves to 1.64 μg/mg dry weight (1.23 to 1.93 μg/mg dry weight) in the explants (Fig. 6C). This confirmed the substantial capacity for cell infiltration 1 year after implantation, which was further verified by histology showing the presence of cell nuclei throughout the entire valve up to the free edges of the valve leaflets (Fig. 5D and fig. S9).

Low αSMA expression of infiltrating cells and full endothelialization of TEHVs after 1 year in vivo

In all TEHVs examined (n = 9), abundant cellular repopulation was observed. Staining for αSMA was performed to evaluate the contractile capacity of the infiltrating cells, and vimentin staining was used to assess the phenotypical state of the interstitial-like cells. In all assessed valves, substantial amounts of αSMA-positive cells were found in the wall, suggesting a functional remodeling toward the layered vascular structure. On the contrary, in all TEHVs, no or only very few αSMA-positive cells were detected in the leaflets and in the hinge areas (Fig. 5F) except for one specimen with signs of endocarditis (valve J; fig. S15) as well as the malpositioned valve G, which was excluded from the main analysis (figs. S4 and S16). A heterogeneous distribution of vimentin-positive cells was identified in the wall, hinge, and leaflet area of the valves (Fig. 5G). Moreover, a homogeneous endothelialization was evident in all valves (n = 9) as seen from CD31 staining and SEM (Fig. 5, H and I). The valves presented a smooth surface with oriented and elongated cells as well as the typical endothelial cobblestone morphology. In one case (valve J), SEM analysis of the TEHV suggested the presence of a recent bacteremia (endocarditis) (fig. S15F). This was also the only case in which αSMA-positive cells were present in the leaflet area, although this did not affect valve functionality throughout the follow-up course (fig. S15D). Together, the presented histological results highlighted the different remodeling processes that occur upon TEHV implantation including cellular infiltration and differentiation, collagen and elastin deposition, and functional remodeling toward a native-like tissue architecture (fig. S17).

DISCUSSION

Here, we provide long-term evidence in a clinically relevant and regulatory accepted large-animal model that computationally inspired designs can successfully and consistently guide physiological remodeling and preserve functionality of living TEHVs. Beyond previous studies in which we established the in vitro culture procedure and computational framework to predict tissue remodeling, this comprehensive work validates the relevance of an integrated in silico, in vitro, and in vivo bioengineering approach as a basis for the safe and efficient clinical translation of heart valve TE.

Computational modeling and mechanistic understanding of success and failure

Computational modeling has been a critical factor in obtaining the favorable outcome of our study, both in terms of proposing an analytical

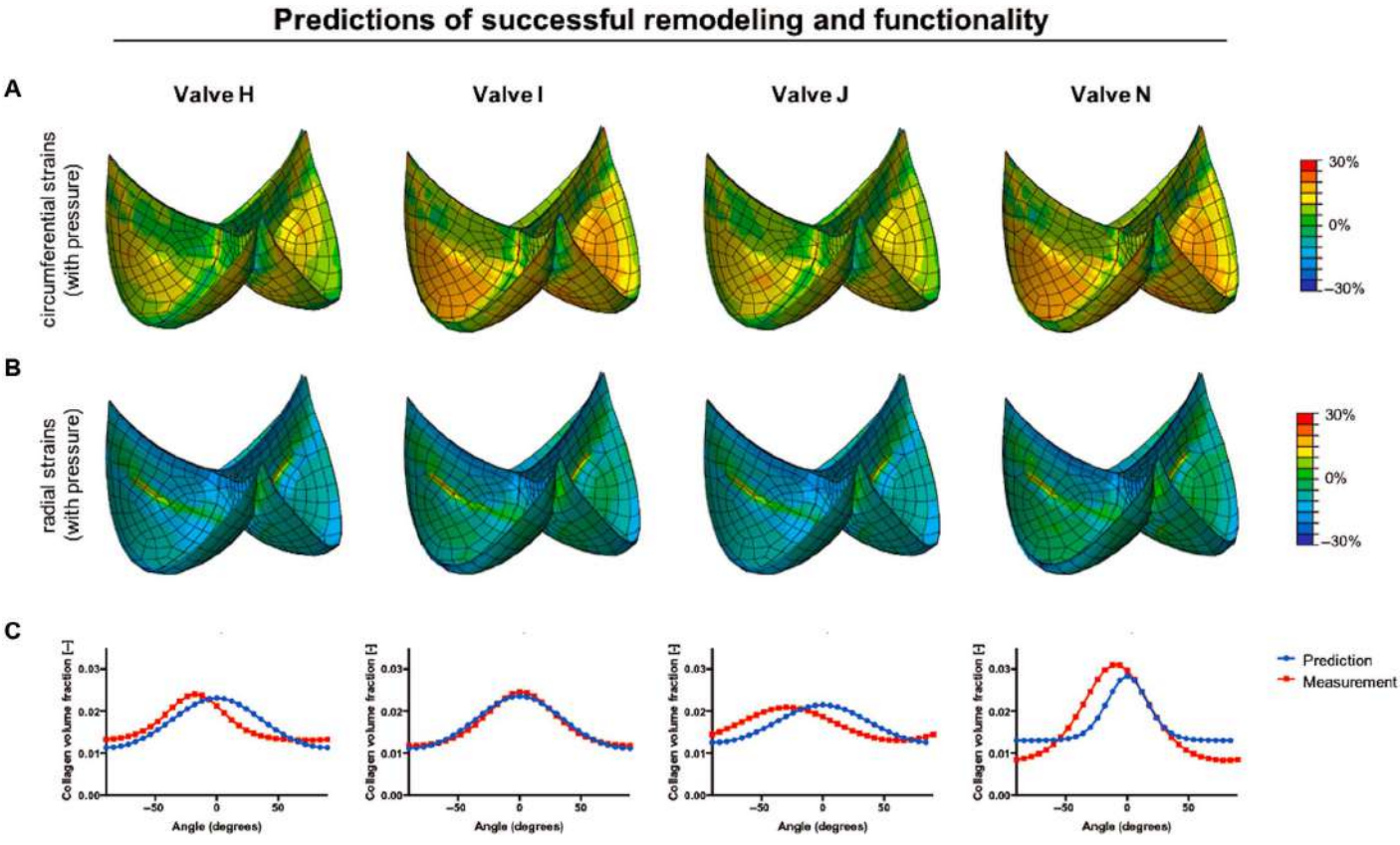

Fig. 4. Computational predictions of valve remodeling based on valve-specific tissue properties at explantation. (**A**) Circumferential and (**B**) radial strains predicted for the different valves during hemodynamic loading. (**C**) Measured (red) and predicted (blue) collagen architecture for each valve.

valve design that can prevent excessive leaflet retraction and in the prediction and fundamental understanding of the observed remodeling of TEHVs. Several previous preclinical studies have demonstrated that remodeling of TEHVs does not naturally lead to a desired outcome (*11*, *12*, *15*, *17*, *18*, *20*–*22*). Consequently, because of the strong interdependency of mechanics and tissue remodeling, mechanical models that can predict the relevant biological mechanisms are extremely valuable in understanding the adaptation of engineered cardiovascular tissues and proposing solutions for how to improve their performance. The present study is an encouraging example of integrating computational modeling, TE, and long-term in vivo validation to develop native-like valve replacements. Moreover, with our computational framework, we identified major determinants in the remodeling process and predicted both success (valves H, I, J, and N) and failure (valve G) of our TEHVs in line with the observed experimental outcomes. Cell contractility and hemodynamics were predicted to play a pivotal role in valve remodeling, emphasizing that preservation of functionality can only be expected for low degrees of contractility combined with physiological hemodynamic conditions.

Computationally inspired valve design and long-term functionality

In contrast to the previously observed general phenomena of leaflet retraction leading to valvular dysfunction (*11*, *12*, *15*, *17*, *18*, *20*–*22*), here, functionality was preserved in all valves over the period of 1 year except for one specimen. This TEHV specimen (valve E) presented with a steady increase in valve insufficiency in several control examinations starting at 3 months and met the endpoint criteria (regurgitation fraction >30% in two consecutive MRI exams) 6 months after implantation. Retrospectively, this valve macroscopically appeared to have a more premature tissue formation during the process of valve culture, and therefore should have been excluded from implantation (although it passed the in vitro valve functionality test). From the clinical translation point of view, this emphasizes the importance of stringent quality and release criteria and highly regulated processes (Good Manufacturing Practice) toward clinical trials (*1*).

The other nine valves showed good functionality with a mean regurgitation fraction below 14% after 1 year, representing a clinically irrelevant, trivial to mild insufficiency. These results substantially differ from our previous studies based on TEHVs manufactured with identical in vitro procedures but without analytical geometries. Already after 24 weeks, Driessen-Mol *et al.* (*15*) showed moderate to severe insufficiency in all TEHVs, and after 1 year, Schmitt *et al.* (*22*) reported severe insufficiency in 80% of TEHVs. To comply with current International Organization for Standardization (ISO) norms for heart valve prostheses in the low-pressure circulation, regurgitation up to 20% is acceptable. All TEHVs investigated in this study except valve E, which was explanted at 6 months, met this criterion at all stages of testing (after production, after implantation, and at explantation), confirming the clinical-grade functional competence of our TEHVs throughout the 1-year in vivo period and the impact of the computationally inspired change in valve design on the overall outcome.

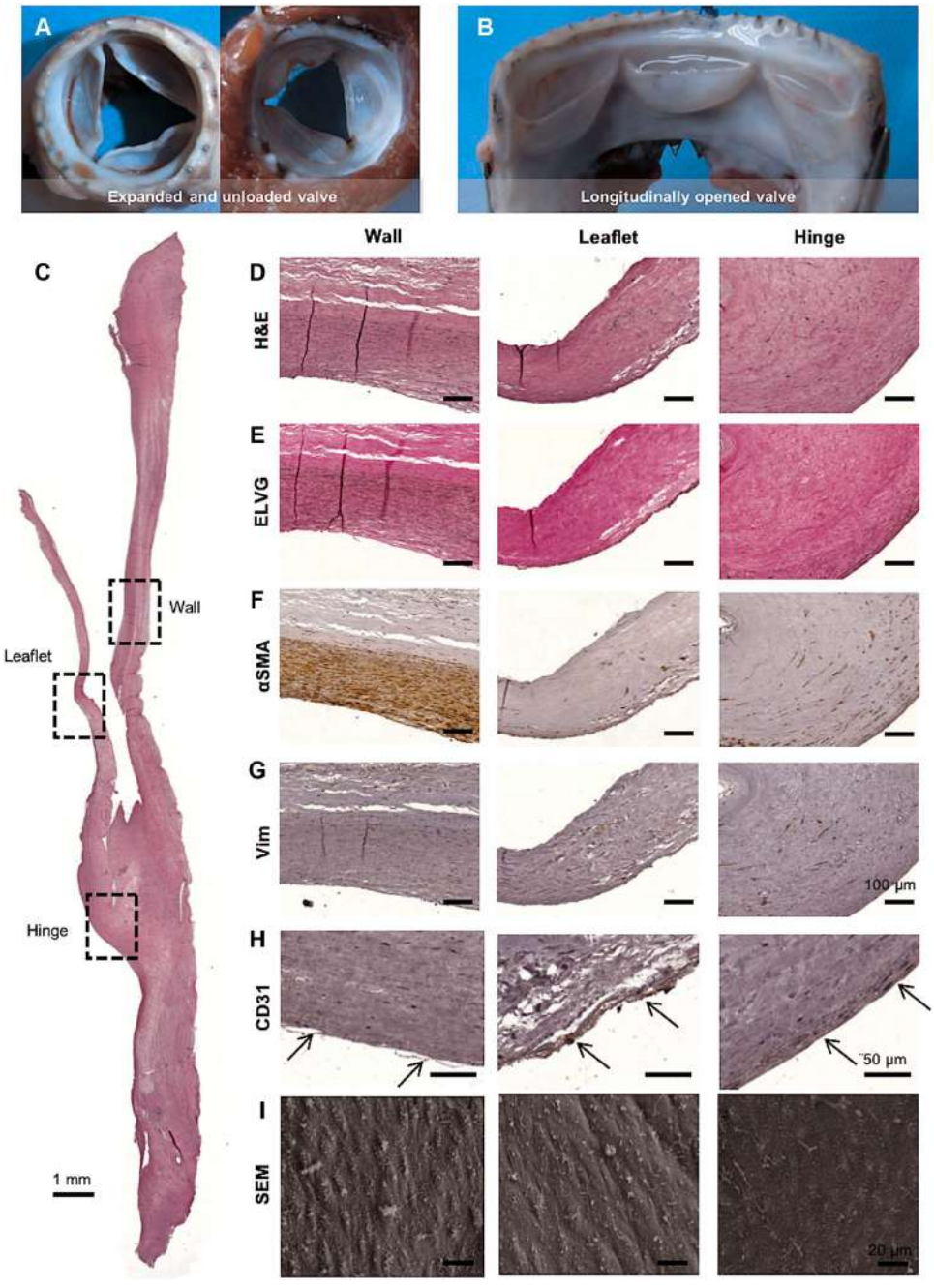

Fig. 5. Postmortem histological analyses of an exemplary TEHV explant after 1 year in vivo (valve N). (**A**) Gross images of the valve after harvest with distal and proximal views of the fully expanded unloaded valve and (**B**) of the three leaflets after the valve was cut open longitudinally through one of the commissural points. (**C**) Hematoxylin and eosin (H&E) staining of the longitudinal transection of entire valve and (**D**) of the higher magnification of the insets (black boxes) from the wall, leaflet, and hinge areas (scale bars, 100 μm). (**E** to **H**) Stainings for Elastica van Gieson (ELVG), αSMA, vimentin, and CD31 (arrows indicate endothelial cells) in the wall, leaflet, and hinge areas (scale bars, 100 μm). (**I**) Scanning electron microscopy (SEM) analysis of the wall, leaflet, and hinge surfaces of the explanted TEHV (scale bars, 20 μm).

Toward native-like tissue remodeling

In terms of matrix composition, the amount of key ECM constituents such as HYP was significantly increased in the TEHVs after 1-year follow-up in vivo when compared to the nonimplanted controls and was comparable to those of native valves (*15*), demonstrating the potential to remodel toward native-like tissue architectures. Elastic fibers could be detected in most of the samples, mainly in the wall and hinge regions. This is remarkable because elastic fibers are typically formed in young, developing tissues, but there is little or no synthesis in adults (*39*). Valvular elastin deposition increases with the closure of the foramen ovale and the separation of the pulmonary and systemic circulation after birth and throughout childhood, demonstrating the impact of hemodynamics on the regulation of elastin production (*40*), proper valvulogenesis (*41*, *42*), and ECM synthesis (*43*). This indicates that hemodynamic loading of our TEHVs in combination with cellular repopulation and differentiation toward the native-like phenotypes may be key factors in the elastogenesis observed.

When compared to the nonimplanted controls, the degree of collagen alignment was significantly higher after 1 year in vivo but still lower when compared to the alignment in native heart valves. We hypothesize that this relatively low collagen alignment was also responsible for the lower radial stretch in our TEHVs compared to native valves. However, this did not negatively affect valve functionality. Human fetal heart valves also feature limited collagen alignment (*40*, *44*), indicating that the collagen architecture observed in the TEHVs may be in line with early-phase collagen maturation. In addition, our computational simulations showed that this amount of alignment is to be expected given the current combination of valve design, material properties, and hemodynamic conditions.

Leaflet lengths decreased over the 1-year implantation period. The mode of shortening observed was fundamentally different than previous work in which leaflet retraction was driven by αSMA-positive cells and leaflet-wall fusion (*15*, *22*), both of which were absent in the present study. As predicted by the computational models, the decrease in leaflet length primarily occurred in the coaptation area (>70% of the observed total reduction in leaflet length; as confirmed by ICE) and is likely the result of functional remodeling toward a more physiological coaptation length. Leaflet length was observed to reach an equilibrium within the first 6 months of implantation (as confirmed by echo and predicted by the computational model), indicating that any further reduction in length after the 1-year follow-up is rather unlikely.

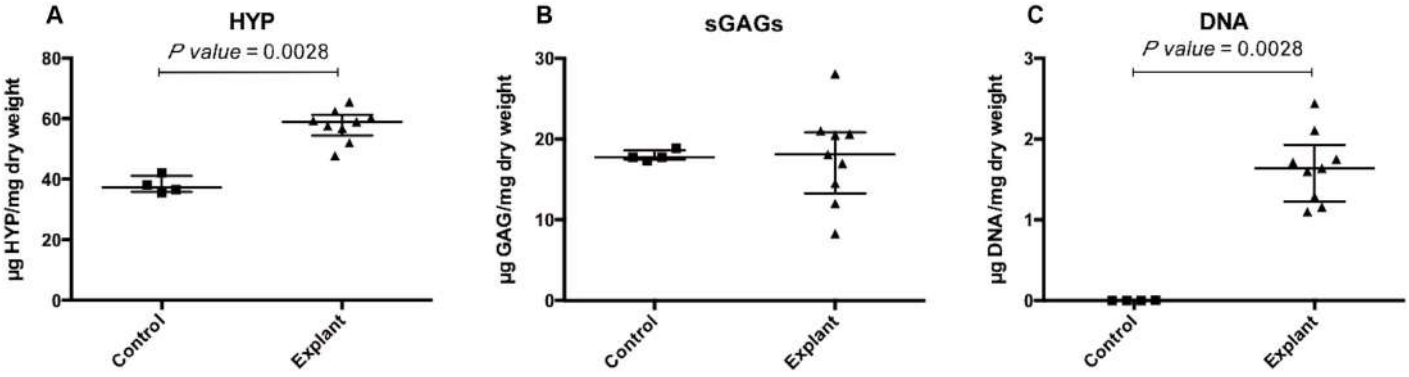

Fig. 6. Biochemical tissue remodeling analysis. (**A** to **C**) HYP, sGAGs, and DNA content in the nonimplanted control valves and explants. Data are median with the IQR. Groups were compared using unpaired, two-tailed Mann-Whitney tests.

Histological evaluation and DNA quantification confirmed substantial host cell repopulation throughout the entire TEHV during the study period of 1 year after implantation. This indicated that the TEHVs carry a sufficient remodeling and regeneration capacity, which is of paramount importance to maintain valve functionality. However, the DNA content in the explants after 1 year in vivo was still lower than that in native ovine leaflets (*15*). This did not compromise TEHV performance, which is in line with recent literature suggesting that the amount of native DNA does not dictate functional tissue remodeling properties (*45*). The amount of DNA in the explants was comparable with the amount of DNA found in human pulmonary leaflets (*46*).

A critical factor in maintaining proper valve functionality is to limit the number of contractile cells, as shown by computational simulations. In our previous studies (*15*, *22*), valvular insufficiency was mainly caused by leaflet retraction due to the contractile phenotype of the infiltrating αSMA-positive cells. Here, αSMA-positive cells were practically absent in the explanted leaflets, similar to native valve leaflets in which valvular interstitial cells (VICs) are usually in a quiescent state to maintain normal valve physiology. However, in the setting of pathological conditions and/or abnormal hemodynamic cues, VICs become activated, gaining αSMA positivity and increasing migration, proliferation, and remodeling potential (*47*). Therefore, it can be hypothesized that the computational modeling–inspired valve design used here provides more physiological mechanical environments to the infiltrating cells, promoting their quiescent state and, therefore, minimizing the expression of a contractile phenotype (*27*).

Relevance and implications for the field: Addressing a central roadblock toward clinical translation

To date, safe clinical translation of most heart valve TE technologies has been prevented by valvular dysfunction associated with adverse valve remodeling (leaflet thickening, irregularities, delamination, and leaflet retraction). These undesired results have been reported independently of the TE methodologies used for the manufacturing of the valve, ranging from classical autologous cell-based in vitro concepts (*17*, *20*, *21*) and off-the-shelf engineered matrices to fully synthetic polymer-based in situ strategies (*10*–*12*, *15*, *18*, *22*). Most of the data report continuous deterioration of valve function starting at around 8 to 12 weeks after implantation due to leaflet retraction (*10*–*12*, *15*, *17*, *18*, *20*–*22*). This phenomenon has been reported to be driven primarily by the presence of αSMA-positive cells in the TEHV leaflets that contract during the remodeling process. Here, using a computational modeling–inspired design, valve functionality was preserved throughout 1 year with almost no αSMA-positive, contracting cells detected in the explanted TEHV leaflets. When considering that the manufacturing process of the valves used in the current study was identical to our previous preclinical large-animal studies (*15*, *22*), the computational modeling–inspired valve geometry is recognized as a key factor responsible for this favorable outcome. Still, it is important to note that valve functionality and remodeling are determined by the combination of valve geometry, material properties, and hemodynamic loading conditions. Although each of these parameters may dominate the ultimate outcome, we propose that optimization of both valve geometry and material properties in consideration of the hemodynamic conditions is essential for improving TEHV performance.

Long-term data for TE heart valves remain limited. Our results are a step toward the development of a clinically relevant approach. In this context, we also recently reported results using a fully synthetic, cell-free biodegradable polymer as a starter material (*10*). Although the polymer-based approach is attractive in terms of low costs and manufacturing logistics, it is different from the current study because remodeling is completely based on slowly degrading (>1 year) synthetic materials and therefore is fully dependent on post-implantation tissue formation. Accordingly, long-term safety is still unclear, and further in vivo validation is necessary until the polymer is completely resolved (*10*). From the clinical translational point of view, TEHVs generated in vitro from competent, homologous neomatrix formed before the time of implantation conceptually provide increased clinical safety profiles.

Limitations

The present study has several limitations. We used a single, 1-year follow-up endpoint for the assessment of the architecture and macroscopic appearance of the TEHVs. Consequently, temporal architectural and geometrical changes during the extensive tissue remodeling process were captured only indirectly by extensive multimodal imaging (ICE and MRI), which was performed to ensure that potential adverse changes affecting valve structure and functionality could be detected immediately. It would be interesting to assess the functionality of our TEHVs beyond the study period to further investigate additional remodeling phenomena, such as the formation of the typical trilayered leaflet structure, which was not detected in most of the TEHVs 1 year after implantation. One of the explants (valve H) displayed more advanced characteristics similar to the native-like trilayered structure, composed of a dense collagenous matrix on the fibrosa side, a less dense collagenous matrix in the central region, and elastin expression on the ventricularis. In vivo evaluation beyond 1 year would be important to

assess potential degenerative processes, which were absent from the current observation period. As such, special attention needs to be paid to the longer-term behavior of the observed microcalcifications in response to the residual scaffold remnants. Further optimization of scaffold technology and composition, such as tuning the poly-4-hydroxybutyrate (P4HB) concentration, may reduce the occurrence of such microcalcifications.

Our computational framework also has limitations. Because models are inherently a simplification of reality, we only included the subset of tissue components that are most strongly associated with mechanically induced tissue remodeling. We validated the individual aspects of the model on several cases of soft tissue remodeling featuring different geometries and loading conditions in previous works (*34*, *36*–*38*). We derived the material parameters associated with the stiffness of collagen fibers from equibiaxial tensile tests. Using only a single deformation mode has limitations regarding the accuracy of material parameters, particularly for strongly anisotropic tissues. However, we hypothesize that the current approach reasonably captures the material behavior, because of the relatively isotropic nature of our tissues and the observation that the combination of fitted parameters accurately captures the measured stress-strain curves. Finally, the detection of elastin in our valves is a remarkable finding warranting additional research to further elucidate the exact mechanism(s) of elastogenesis and elastin maturation (*48*), which was beyond the scope of this study.

Here, we provide long-term in vivo evidence that a computationally inspired heart valve design can successfully and consistently guide physiological remodeling and preserve functionality of TEHVs in sheep. The current study demonstrates the relevance of an integrated in silico, in vitro, and in vivo bioengineering approach as a basis for the safe and efficient clinical translation of heart valve TE. From the clinical point of view, when compared to the well-established and predictable performance of contemporary valve prostheses (mechanical or bioprosthetic heart valves), the safety of next-generation TEHVs will be critically dependent upon their tissue remodeling behavior. Therefore, a computational modeling–based prediction of valve success or failure may be instrumental in achieving clinical readiness of heart valve TE technologies.

MATERIALS AND METHODS

Study design

The main objective of this study was to test the hypothesis that integration of a computationally inspired heart valve design can guide tissue remodeling and ensure long-term functionality in TEHVs in vivo. After manufacturing the TEHVs (n = 15), computational modeling was used to predict the in vivo remodeling process. Thereafter, TEHVs (n = 11) were implanted as pulmonary valve replacements in a clinically relevant sheep model using minimally invasive techniques and were followed up for 1 year using longitudinal ICE and cardiac MRI assessments. The other TEHVs (n = 4) served as nonimplanted controls. Functional valve performance (regurgitation fraction, pressure gradient, and insufficiency grade) and the absence of degeneration and thromboembolism were evaluated. Subsequently, computational predictions of in vivo TEHV remodeling and functionality, based on either average initial properties or individual explant properties, were compared to understand valve outcomes. As a measure of the remodeling process and its features, comprehensive postmortem analysis of the TEHVs was performed for the following parameters: (i) the infiltration of host cells/cellular repopulation; (ii) expression of the native-like cellular phenotypes; (iii) ECM (collagen and elastin) deposition, maturation, and organization (orientation); (iv) ECM quantification; (v) presence of scaffold remnants; (vi) calcification; and (vii) functional adaptations in valve geometry (sinus formation and adaptation of leaflet length and thickness).

TEHV manufacturing

TEHVs (n = 15; valves A to O) were cultured as previously described (*15*). In brief, tri-leaflet heart valves were obtained from polyglycolic acid meshes (Cellon), sewn into self-expandable nitinol stents (PFM Medical AG), and coated with 1.75% P4HB (TEPHA Inc.). Primary isolated ovine vascular-derived cells were seeded using fibrin as a cell carrier and cultured for 4 weeks in an in-house developed bioreactor system, including geometrical constraints to shape the tissue into the suggested design (*33*). After 4 weeks of culture, all TEHVs (n = 15) were decellularized as described by Dijkman *et al.* (*35*). After sterilization, they were stored at 4°C until further use. Detailed description of the manufacturing process is available in the "Manufacturing of tissue-engineered heart valves (TEHVs)" section of Supplementary Materials and Methods.

In vitro functionality assessment

The functionality of all TEHVs (n = 15) was tested before implantation using a hydrodynamic pulsatile test system (HDT-500, BDC Laboratories). Physiological flows and pressures were generated to mimic in vivo situations. On the basis of the recorded data using the corresponding Statys software (BDC Laboratories), regurgitation fractions were quantified and discriminated between closing and leakage volume, expressed as a percentage of the stroke volume. Details on the evaluation of valve functionality in vitro are available in the "In vitro functionality assessment" section of Supplementary Materials and Methods.

Animal studies

TEHVs were implanted as pulmonary valve replacement via transcatheter-based jugular access in 11 adult female sheep (strain, gray horned heathes; provider, Kyritz) using angiography and hemodynamic measurements, exposing the TEHVs to physiological pressure and flow conditions during the implantation period. To assess TEHV functionality, all sheep were followed up for 1 year by ICE and cardiac MRI. In addition, cardiac CT was performed before and after implantation and before explantation. At explantation, hemodynamic measurements and angiography were repeated. Anesthesia and implantation were carried out as previously described (*22*) and as detailed in the "Anesthesia" and "Implantation and deployment of TEHVs" sections of Supplementary Materials and Methods.

The in vivo study was approved by the local authorities (Regional Office for Health and Social Affairs Berlin, LAGeSo, Berlin; approval no. G0111/11). Animals were treated in accordance with the guidelines of the European and German Societies of Laboratory Animal Science (FELASA, GV-SOLAS) and to the ARRIVE guidelines (Animal Research: Reporting of In vivo Experiments).

Hemodynamics and imaging

For the assessment of hemodynamics, guidance of implantation, and TEHV performance analysis, clinically relevant multimodal imaging comprising angiography, CT, ICE, and cardiac MRI was used (see the "Hemodynamics," "Angiography," and "In vivo assessment of TEHVs" sections of Supplementary Materials and Methods for further details).

Computational prediction of valve functionality and remodeling

Prediction of initial in vivo strains

The initial mechanical behavior of the valves was predicted using computational modeling as described previously (*32*, *33*). In short, the valve geometry was described according to Hamid *et al.* (*49*) and equaled the geometry imposed on the TEHVs via the geometrical constraints described above. Material parameters were fitted to the average biaxial tensile test results of the four control valves. Finally, a pressure of 15 mmHg was applied to the arterial side of the valve. Leaflet thickness was varied between 50 and 150% of the average thickness of the control valves to accommodate variations across the implanted valves. Simulations were performed using the commercial finite element package Abaqus (Abaqus 6.14, Dassault Systèmes Simulia Corp.) using the user-defined subroutine UMAT. Detailed description of the methodologies used is reported in the "Computational prediction of valve functionality and remodeling" section of Supplementary Materials and Methods.

Prediction of in vivo remodeling from initial tissue properties

Starting from the geometry and average material properties of the control valves, in vivo remodeling of the TEHVs was predicted using our recently developed computational framework, describing the processes of cell orientation, reorientation, cell contractility, cell-mediated collagen contraction, and collagen turnover in response to mechanical stimuli (see the "Computational prediction of valve functionality and remodeling" section of Supplementary Materials and Methods for additional information) (*34*, *36*–*38*). Dynamic pulmonary loading conditions were applied, assuming that the maximum trans-valvular pressure difference equals 15 mmHg. Leaflet thickness was varied between 50 and 150% of the average thickness of the control valves. In addition, the contractility of the cells was varied between the original value in (*37*), mostly resembling a myofibroblast phenotype, and 20% of the original value, resembling a fibroblast phenotype with low αSMA expression.

Predicting differences in outcome between explants

Animal-specific simulations of the remodeling process were performed, where the material properties for each simulation were derived from the mechanical tests of the corresponding explant. These material parameters only concerned the stiffness parameters of the collagen fibers; the initial collagen distribution (before in vivo remodeling) was assumed to be isotropic in all cases. Measured differences in leaflet thickness were incorporated, but no differences in initial valve geometry were assumed, because this was imposed via the geometrical constraints before implantation.

Quantification of collagen alignment

To objectively compare the different collagen architectures derived from the CNA stainings and predicted by the computational model, the following periodic function was fitted through each of the histograms

$$\varphi_{cf} = A\exp\left[\frac{\cos[2(\gamma-\alpha)]+1}{\beta}\right] + C \qquad (1)$$

where γ is the angle with respect to the main orientation α of the collagen network, β is a measure for the dispersity, and a constant C was added because this resulted in better fits to the data. The ratio of the maximum and minimum of the fit was determined as an objective quantitative measure for collagen anisotropy.

Postmortem remodeling analysis

Histology and immunohistochemistry

Tissue morphology and cell infiltration were assessed using H&E, and Masson Goldner staining was performed. Next, Elastica van Gieson staining was carried out to evaluate collagen and elastic fiber distribution, whereas von Kossa staining was used to detect calcification. Immunohistochemistry for αSMA vimentin and CD31 was used to assess cell marker expression. Further details on the materials and methods used for these analyses are available in the "Histology and immunohistochemistry" section of Supplementary Materials and Methods.

Scanning electron microscopy

To assess TEHV surface morphology and to evaluate the degree of endothelialization of the TEHVs, representative tissue samples of the explanted TEHVs (n = 10) and control valves (n = 4) were fixed in 2% glutaraldehyde (Sigma), dehydrated in a graded series of ethanol (70, 80, 90, and 100%), and platinum-sputtered (CCU-010 HV Compact Coating Unit, Safematic GmbH). SEM preparation and analysis were performed at the Center for Microscopy and Image Analysis of the University of Zurich (Zurich, Switzerland). Pictures were acquired using a Zeiss Supra 50 VP SEM with an acceleration voltage of 10 kV.

Leaflet dimensions

The distance of the hinge region toward the end of the stent was measured to define the leaflet position relative to the wall. The total length of the leaflet through the longitudinal symmetry axis, from the hinge to the free edge, was determined to quantify changes in leaflet length over time. Measurements were taken from three leaflets per control valve (n = 4), as well as from the explanted valves (n = 9), using digital calipers (CD-15CPX, Mitutoyo). Leaflet thickness was measured using a digital microscope (VHX-500FE, Keyence).

Collagen orientation

Detailed description is available in the "Assessment of collagen orientation" section of Supplementary Materials and Methods.

Biomechanical analyses

Mechanical properties of all control valves (n = 4) and explants (n = 9) were analyzed by using a biaxial tensile tester (BioTester, 2.5 N load cell; CellScale) in combination with LabJoy software (V8.01, CellScale) (see the Supplementary Materials for further details). The obtained data were used as input for the computational simulations.

Quantitative tissue analyses

The total amount of DNA, sGAGs, and HYP of explants (n = 9) and control valves (n = 4) was analyzed using predefined biochemical assays as previously described (*15*, *35*). Values were represented with respect to the dry weight of the samples.

Statistics

Data in the text are represented as means ± SD unless stated otherwise. The biochemical analyses, leaflet dimensions of the explants, and collagen anisotropy of the image analyses were evaluated by an unpaired, two-tailed Mann-Whitney test using GraphPad Prism (version 6). Leaflet length based on ICE data was evaluated using a two-tailed Wilcoxon matched-pairs signed rank test in IBM SPSS Statistics (version 22) software. In line with nonparametric testing, graphical data were represented as the median with the IQR, where statistical significance was considered for $P < 0.05$.

SUPPLEMENTARY MATERIALS

www.sciencetranslationalmedicine.org/cgi/content/full/10/440/eaan4587/DC1
Materials and Methods
Fig. S1. Schematic overview of study concept.
Fig. S2. Gross and histological characterization of a control TEHV.
Fig. S3. Overview of the clinical-grade percutaneous implantation system and the multimodality imaging protocols to assess TEHV positioning, functionality, and performance throughout the study.
Fig. S4. Computational predictions of valve remodeling and postmortem analysis of valve G, which was malpositioned upon implantation.
Fig. S5. Longitudinal cardiac MRI flow measurements for the assessment of TEHV function and regurgitation fraction over 1 year.
Fig. S6. Postmortem analyses of valve E explanted after 6 months in vivo.
Fig. S7. Additional results on the computational predictions of in vivo strains and valve remodeling based on initial tissue properties.
Fig. S8. Analysis of collagen alignment.
Fig. S9. Histological evaluation of cellular infiltration in a representative valve (valve N) using Masson Goldner staining.
Fig. S10. Evaluation of elastogenesis and neosinus formation.
Fig. S11. Assessment of leaflet length and position.
Fig. S12. Evaluation of calcification in different explants with von Kossa staining.
Fig. S13. Histological evaluation of the inflammatory response using H&E staining.
Fig. S14. Evaluation of leaflet remodeling using Elastica van Gieson staining.
Fig. S15. Postmortem analyses of valve J explanted after 1 year in vivo.
Fig. S16. Immunohistochemical analysis for presence and distribution of αSMA-positive cells in valve G.
Fig. S17. Schematic representation depicting the functional remodeling process within the TEHV.
Table S1. In vitro TEHV functionality before implantation.
Table S2. Animal characteristics.
Table S3. Pulmonary dimensions and hemodynamics before and after implantation.
Table S4. Functional long-term catheter data (invasive hemodynamic measurements) of TEHVs at baseline and after 1 year.
Table S5. Functional ICE data of TEHVs at baseline and after 1 year.
Table S6. Functional MRI data of TEHV insufficiency at baseline and after 1 year.
Table S7. Leaflet thickness in the explants.
Movie S1. In vitro TEHV testing.
Movie S2. Angiography after TEHV implantation.
Movie S3. ICE after implantation.
Movie S4. Color-coded ICE after implantation.
Movie S5. ICE at 6-month follow-up.
Movie S6. Color-coded ICE at 6-month follow-up.
Movie S7. ICE at 12-month follow-up.
Movie S8. Color-coded ICE at 12-month follow-up.
References (*50*–*52*)

REFERENCES AND NOTES

1. M. Y. Emmert, E. S. Fioretta, S. P. Hoerstrup, Translational challenges in cardiovascular tissue engineering. *J. Cardiovasc. Transl. Res.* **10**, 139–149 (2017).
2. M. H. Yacoub, J. J. M. Takkenberg, Will heart valve tissue engineering change the world? *Nat. Clin. Pract. Cardiovasc. Med.* **2**, 60–61 (2005).
3. E. Rabkin-Aikawa, J. E. Mayer, F. J. Schoen, Heart valve regeneration. *Adv. Biochem. Eng. Biotechnol.* **94**, 141–179 (2005).
4. M. K. Sewell-Loftin, Y. W. Chun, A. Khademhosseini, W. D. Merryman, EMT-inducing biomaterials for heart valve engineering: Taking cues from developmental biology. *J. Cardiovasc. Transl. Res.* **4**, 658–671 (2011).
5. J. Fernández Esmerats, J. Heath, H. Jo, Shear-sensitive genes in aortic valve endothelium. *Antioxid. Redox Signal.* **25**, 401–414 (2016).
6. T. Kaneko, L. H. Cohn, S. F. Aranki, Tissue valve is the preferred option for patients aged 60 and older. *Circulation* **128**, 1365–1371 (2013).
7. R. Henaine, F. Roubertie, M. Vergnat, J. Ninet, Valve replacement in children: A challenge for a whole life. *Arch. Cardiovasc. Dis.* **105**, 517–528 (2012).
8. R. Langer, J. P. Vacanti, Tissue engineering. *Science* **260**, 920–926 (1993).
9. P. E. Dijkman, A. Driessen-Mol, L. M. de Heer, J. Kluin, L. A. van Herwerden, B. Odermatt, F. P. T. Baaijens, S. P. Hoerstrup, Trans-apical versus surgical implantation of autologous ovine tissue-engineered heart valves. *J. Heart Valve Dis.* **21**, 670–678 (2012).
10. J. Kluin, H. Talacua, A. I. P. M. Smits, M. Y. Emmert, M. C. P. Brugmans, E. S. Fioretta, P. E. Dijkman, S. H. M. Söntjens, R. Duijvelshoff, S. Dekker, M. W. J. T. Janssen-van den Broek, V. Lintas, A. Vink, S. P. Hoerstrup, H. M. Janssen, P. Y. W. Dankers, F. P. T. Baaijens, C. V. C. Bouten, In situ heart valve tissue engineering using a bioresorbable elastomeric implant—From material design to 12 months follow-up in sheep. *Biomaterials* **125**, 101–117 (2017).
11. J. Reimer, Z. Syedain, B. Haynie, M. Lahti, J. Berry, R. Tranquillo, Implantation of a tissue-engineered tubular heart valve in growing lambs. *Ann. Biomed. Eng.* **45**, 439–451 (2017).
12. Z. Syedain, J. Reimer, J. Schmidt, M. Lahti, J. Berry, R. Bianco, R. T. Tranquillo, 6-Month aortic valve implantation of an off-the-shelf tissue-engineered valve in sheep. *Biomaterials* **73**, 175–184 (2015).
13. M. Y. Emmert, B. Weber, P. Wolint, L. Behr, S. Sammut, T. Frauenfelder, L. Frese, J. Scherman, C. E. Brokopp, C. Templin, J. Grünenfelder, G. Zünd, V. Falk, S. P. Hoerstrup, Stem cell–based transcatheter aortic valve implantation: First experiences in a pre-clinical model. *JACC Cardiovasc. Interv.* **5**, 874–883 (2012).
14. M. Y. Emmert, B. Weber, L. Behr, T. Frauenfelder, C. E. Brokopp, J. Grünenfelder, V. Falk, S. P. Hoerstrup, Transapical aortic implantation of autologous marrow stromal cell-based tissue-engineered heart valves: First experiences in the systemic circulation. *JACC Cardiovasc. Interv.* **4**, 822–823 (2011).
15. A. Driessen-Mol, M. Y. Emmert, P. E. Dijkman, L. Frese, B. Sanders, B. Weber, N. Cesarovic, M. Sidler, J. Leenders, R. Jenni, J. Grünenfelder, V. Falk, F. P. T. Baaijens, S. P. Hoerstrup, Transcatheter implantation of homologous "off-the-shelf" tissue-engineered heart valves with self-repair capacity: Long-term functionality and rapid in vivo remodeling in sheep. *J. Am. Coll. Cardiol.* **63**, 1320–1329 (2014).
16. M. Y. Emmert, B. Weber, L. Behr, S. Sammut, T. Frauenfelder, P. Wolint, J. Scherman, D. Bettex, J. Grünenfelder, V. Falk, S. P. Hoerstrup, Transcatheter aortic valve implantation using anatomically oriented, marrow stromal cell-based, stented, tissue-engineered heart valves: Technical considerations and implications for translational cell-based heart valve concepts. *Eur. J. Cardiothorac. Surg.* **45**, 61–68 (2014).
17. D. Schmidt, P. E. Dijkman, A. Driessen-Mol, R. Stenger, C. Mariani, A. Puolakka, M. Rissanen, T. Deichmann, B. Odermatt, B. Weber, M. Y. Emmert, G. Zund, F. P. T. Baaijens, S. P. Hoerstrup, Minimally-invasive implantation of living tissue engineered heart valves: A comprehensive approach from autologous vascular cells to stem cells. *J. Am. Coll. Cardiol.* **56**, 510–520 (2010).
18. B. Weber, P. E. Dijkman, J. Scherman, B. Sanders, M. Y. Emmert, J. Grünenfelder, R. Verbeek, M. Bracher, M. Black, T. Franz, J. Kortsmit, P. Modregger, S. Peter, M. Stampanoni, J. Robert, D. Kehl, M. van Doeselaar, M. Schweiger, C. E. Brokopp, T. Walchli, V. Falk, P. Zilla, A. Driessen-Mol, F. P. T. Baaijens, S. P. Hoerstrup, Off-the-shelf human decellularized tissue-engineered heart valves in a non-human primate model. *Biomaterials* **34**, 7269–7280 (2013).
19. B. Weber, J. Scherman, M. Y. Emmert, J. Gruenenfelder, R. Verbeek, M. Bracher, M. Black, J. Kortsmit, T. Franz, R. Schoenauer, L. Baumgartner, C. Brokopp, I. Agarkova, P. Wolint, G. Zund, V. Falk, P. Zilla, S. P. Hoerstrup, Injectable living marrow stromal cell-based autologous tissue engineered heart valves: First experiences with a one-step intervention in primates. *Eur. Heart J.* **32**, 2830–2840 (2011).
20. T. C. Flanagan, J. S. Sachweh, J. Frese, H. Schnöring, N. Gronloh, S. Koch, R. H. Tolba, T. Schmitz-Rode, S. Jockenhoevel, In vivo remodeling and structural characterization of fibrin-based tissue-engineered heart valves in the adult sheep model. *Tissue Eng. Part A* **15**, 2965–2976 (2009).
21. D. Gottlieb, T. Kunal, S. Emani, E. Aikawa, D. W. Brown, A. J. Powell, A. Nedder, G. C. Engelmayr Jr., J. M. Melero-Martin, M. S. Sacks, J. E. Mayer Jr., In vivo monitoring of function of autologous engineered pulmonary valve. *J. Thorac. Cardiovasc. Surg.* **139**, 723–731 (2010).
22. B. Schmitt, H. Spriestersbach, D. O. h-Icí, T. Radtke, M. Bartosch, H. Peters, M. Sigler, L. Frese, P. E. Dijkman, F. P. T. Baaijens, S. P. Hoerstrup, F. Berger, Percutaneous pulmonary valve replacement using completely tissue-engineered off-the-shelf heart valves: Six-month in vivo functionality and matrix remodelling in sheep. *EuroIntervention* **12**, 62–70 (2016).
23. J. D. Humphrey, Vascular adaptation and mechanical homeostasis at tissue, cellular, and sub-cellular levels. *Cell Biochem. Biophys.* **50**, 53–78 (2008).
24. J. D. Humphrey, D. M. Milewicz, G. Tellides, M. A. Schwartz, Dysfunctional mechanosensing in aneurysms. *Science* **344**, 477–479 (2014).
25. E. Kuhl, Growing matter: A review of growth in living systems. *J. Mech. Behav. Biomed. Mater.* **29**, 529–543 (2014).
26. D. Ambrosi, G. A. Ateshian, E. M. Arruda, S. C. Cowin, J. Dumais, A. Goriely, G. A. Holzapfel, J. D. Humphrey, R. Kemkemer, E. Kuhl, J. E. Olberding, L. A. Taber, K. Garikipati, Perspectives on biological growth and remodeling. *J. Mech. Phys. Solids* **59**, 863–883 (2011).
27. P. Thayer, K. Balachandran, S. Rathan, C. H. Yap, S. Arjunon, H. Jo, A. P. Yoganathan, The effects of combined cyclic stretch and pressure on the aortic valve interstitial cell phenotype. *Ann. Biomed. Eng.* **39**, 1654–1667 (2011).
28. M.-C. Hsu, D. Kamensky, F. Xu, J. Kiendl, C. Wang, M. C. H. Wu, J. Mineroff, A. Reali, Y. Bazilevs, M. S. Sacks, Dynamic and fluid–structure interaction simulations of bioprosthetic heart valves using parametric design with T-splines and Fung-type material models. *Comput. Mech.* **55**, 1211–1225 (2015).

29. C. Martin, W. Sun, Simulation of long-term fatigue damage in bioprosthetic heart valves: Effects of leaflet and stent elastic properties. *Biomech. Model. Mechanobiol.* **13**, 759–770 (2014).
30. J. S. Soares, M. S. Sacks, A triphasic constrained mixture model of engineered tissue formation under in vitro dynamic mechanical conditioning. *Biomech. Model. Mechanobiol.* **15**, 293–316 (2016).
31. J. S. Soares, T. B. Le, F. Sotiropoulos, M. S. Sacks, Modeling the role of oscillator flow and dynamic mechanical conditioning on dense connective tissue formation in mesenchymal stem cell–derived heart valve tissue engineering. *J. Med. Device* **7**, 0409271–0409272 (2013).
32. S. Loerakker, G. Argento, C. W. J. Oomens, F. P. T. Baaijens, Effects of valve geometry and tissue anisotropy on the radial stretch and coaptation area of tissue-engineered heart valves. *J. Biomech.* **46**, 1792–1800 (2013).
33. B. Sanders, S. Loerakker, E. S. Fioretta, D. J. P. Bax, A. Driessen-Mol, S. P. Hoerstrup, F. P. T. Baaijens, Improved geometry of decellularized tissue engineered heart valves to prevent leaflet retraction. *Ann. Biomed. Eng.* **44**, 1061–1071 (2016).
34. S. Loerakker, T. Ristori, F. P. T. Baaijens, A computational analysis of cell-mediated compaction and collagen remodeling in tissue-engineered heart valves. *J. Mech. Behav. Biomed. Mater.* **58**, 173–187 (2016).
35. P. E. Dijkman, A. Driessen-Mol, L. Frese, S. P. Hoerstrup, F. P. T. Baaijens, Decellularized homologous tissue-engineered heart valves as off-the-shelf alternatives to xeno- and homografts. *Biomaterials* **33**, 4545–4554 (2012).
36. S. Loerakker, C. Obbink-Huizer, F. P. T. Baaijens, A physically motivated constitutive model for cell-mediated compaction and collagen remodeling in soft tissues. *Biomech. Model. Mechanobiol.* **13**, 985–1001 (2014).
37. C. Obbink-Huizer, C. W. J. Oomens, S. Loerakker, J. Foolen, C. V. C. Bouten, F. P. T. Baaijens, Computational model predicts cell orientation in response to a range of mechanical stimuli. *Biomech. Model. Mechanobiol.* **13**, 227–236 (2014).
38. T. Ristori, C. Obbink-Huizer, C. W. J. Oomens, F. P. T. Baaijens, S. Loerakker, Efficient computational simulation of actin stress fiber remodeling. *Comput. Methods Biomech. Biomed. Eng.* **19**, 1347–1358 (2016).
39. B. W. Robb, H. Wachi, T. Schaub, R. P. Mecham, E. C. Davis, Characterization of an in vitro model of elastic fiber assembly. *Mol. Biol. Cell* **10**, 3595–3605 (1999).
40. E. Aikawa, P. Whittaker, M. Farber, K. Mendelson, R. F. Padera, M. Aikawa, F. J. Schoen, Human semilunar cardiac valve remodeling by activated cells from fetus to adult: Implications for postnatal adaptation, pathology, and tissue engineering. *Circulation* **113**, 1344–1352 (2006).
41. M. Reckova, C. Rosengarten, A. de Almeida, C. P. Stanley, A. Wessels, R. G. Gourdie, R. P. Thompson, D. Sedmera, Hemodynamics is a key epigenetic factor in development of the cardiac conduction system. *Circ. Res.* **93**, 77–85 (2003).
42. D. Sedmera, T. Pexieder, V. Rychterova, N. Hu, E. B. Clark, Remodeling of chick embryonic ventricular myoarchitecture under experimentally changed loading conditions. *Anat. Rec.* **254**, 238–252 (1999).
43. K.-W. Lee, D. B. Stolz, Y. Wang, Substantial expression of mature elastin in arterial constructs. *Proc. Natl. Acad. Sci. U.S.A.* **108**, 2705–2710 (2011).
44. P. J. A. Oomen, S. Loerakker, D. van Geemen, J. Neggers, M.-J. T. H. Goumans, A. J. van den Bogaerdt, A. J. J. C. Bogers, C. V. C. Bouten, F. P. T. Baaijens, Age-dependent changes of stress and strain in the human heart valve and their relation with collagen remodeling. *Acta Biomater.* **29**, 161–169 (2016).
45. Z. Syedain, J. Reimer, M. Lahti, J. Berry, S. Johnson, R. T. Tranquillo, Tissue engineering of acellular vascular grafts capable of somatic growth in young lambs. *Nat. Commun.* **7**, 12951 (2016).
46. D. van Geemen, A. L. F. Soares, P. J. A. Oomen, A. Driessen-Mol, M. W. J. T. Janssen-van den Broek, A. J. van den Bogaerdt, A. J. J. C. Bogers, M.-J. T. H. Goumans, F. P. T. Baaijens, C. V. C. Bouten, Age-dependent changes in geometry, tissue composition and mechanical properties of fetal to adult cryopreserved human heart valves. *PLOS ONE* **11**, e0149020 (2016).
47. A. C. Liu, V. R. Joag, A. I. Gotlieb, The emerging role of valve interstitial cell phenotypes in regulating heart valve pathobiology. *Am. J. Pathol.* **171**, 1407–1418 (2007).
48. L. Robert, Cell-elastin interaction and signaling. *Pathol. Biol.* **53**, 399–404 (2005).
49. M. S. Hamid, H. N. Sabbah, P. D. Stein, Influence of stent height upon stresses on the cusps of closed bioprosthetic valves. *J. Biomech.* **19**, 759–769 (1986).
50. K. N. Krahn, C. V. C. Bouten, S. van Tuijl, M. A. M. J. van Zandvoort, M. Merkx, Fluorescently labeled collagen binding proteins allow specific visualization of collagen in tissues and live cell culture. *Anal. Biochem.* **350**, 177–185 (2006).
51. M. Bartosch, H. Peters, H. Spriestersbach, D. O. h-Icí, F. Berger, B. Schmitt, A universal delivery system for percutaneous heart valve implantation. *Ann. Biomed. Eng.* **44**, 2683–2694 (2016).
52. P. Lancellotti, C. Tribouilloy, A. Hagendorff, B. A. Popescu, T. Edvardsen, L. A. Pierard, L. Badano, J. L. Zamorano; Scientific Document Committee of the European Association of Cardiovascular Imaging, Recommendations for the echocardiographic assessment of native valvular regurgitation: An executive summary from the European Association of Cardiovascular Imaging. *Eur. Heart J. Cardiovasc. Imaging* **14**, 611–644 (2013).

Acknowledgments: We thank M. Bartosch (Department of Congenital Heart Disease, German Heart Center Berlin, Germany) for developing the minimally invasive delivery system, C. De Simio-Hilton (Department of Surgical Research, University Hospital Zurich, Switzerland) for graphical support, and M. Hilbe (Institute of Veterinary Pathology, Vetsuisse Faculty, University of Zurich, Zurich, Switzerland) for expert advice on histopathologic assessment of the valve specimens. **Funding:** We gratefully acknowledge the funding from the European Union's Seventh Framework Program (FP7/2007-2013) under grant agreement no. 242008. M.Y.E. was supported by the Swiss National Science Foundation, the Swiss Heart Foundation, and the Olga Mayenfisch Foundation. **Author contributions:** S.P.H., F.P.T.B., and F.B. obtained the funding. M.Y.E., B.A.S., S.L., B.S., F.P.T.B., F.B., and S.P.H. designed the study concept. B.A.S., H.S., L.B., and K.B. performed in vivo experiments. S.L. performed the computational modeling. B.S. and E.S.F. performed valve manufacturing and in vitro characterization. M.Y.E., E.S.F., S.E.M., V.L., P.E.D., and L.F. performed postmortem evaluation. M.Y.E., B.A.S., S.L., B.S., H.S., E.S.F., L.B., K.B., S.E.M., V.L., P.E.D., L.F., F.B., F.P.T.B., and S.P.H. acquired and/or analyzed the data. M.Y.E., B.A.S., S.L., B.S., E.S.F., F.B., F.P.T.B., and S.P.H. drafted and/or revised the manuscript for critical content. M.Y.E., B.A.S., S.L., B.S., and S.P.H. wrote the manuscript. Administrative, technical, or supervisory tasks were handled by M.Y.E., B.A.S., S.L., B.S., F.B., F.P.T.B., and S.P.H. **Competing interests:** B.S., S.L., F.P.T.B., and S.P.H. are inventors on patent "Controlling TEHV geometry by using predefined inserts during culture" (WO2015044190 A1) held by Eindhoven University of Technology. This patent covers how the shape of the heart valves can be controlled and maintained during the in vitro culture phase. **Data and materials availability:** All relevant data are available in the manuscript and the Supplementary Materials. Requests for materials should be addressed to simon.hoerstrup@irem.uzh.ch (S.P.H.).

Submitted 18 April 2017
Resubmitted 20 September 2017
Accepted 9 April 2018
Published 9 May 2018
10.1126/scitranslmed.aan4587

Citation: M. Y. Emmert, B. A. Schmitt, S. Loerakker, B. Sanders, H. Spriestersbach, E. S. Fioretta, L. Bruder, K. Brakmann, S. E. Motta, V. Lintas, P. E. Dijkman, L. Frese, F. Berger, F. P. T. Baaijens, S. P. Hoerstrup, Computational modeling guides tissue-engineered heart valve design for long-term in vivo performance in a translational sheep model. *Sci. Transl. Med.* **10**, eaan4587 (2018).

Science Translational Medicine

Computational modeling guides tissue-engineered heart valve design for long-term in vivo performance in a translational sheep model

Maximilian Y. Emmert, Boris A. Schmitt, Sandra Loerakker, Bart Sanders, Hendrik Spriestersbach, Emanuela S. Fioretta, Leon Bruder, Kerstin Brakmann, Sarah E. Motta, Valentina Lintas, Petra E. Dijkman, Laura Frese, Felix Berger, Frank P. T. Baaijens and Simon P. Hoerstrup

Sci Transl Med **10**, eaan4587.
DOI: 10.1126/scitranslmed.aan4587

Modeling remodeling

Patients with valvular heart disease such as aortic stenosis (narrowing of the aortic valve in the heart) receive artificial or bioprosthetic valve replacements, but these have limited longevity and cannot grow with younger patients. Emmert *et al.* used computational modeling to design tissue-engineered heart valves from polymer scaffolds seeded with vascular cells. After 4 weeks of bioreactor culture, the grafts were decellularized before transcatheter implantation in sheep as pulmonary valve replacements. Nine of the 11 grafts remained functional up to 1 year later. Computational modeling predicted that valve leaflets would shorten in vivo during dynamic remodeling before reaching equilibrium, which was confirmed in the sheep. This work suggests that tissue engineering strategies should incorporate computational simulation to lead to more successful outcomes and more predictable clinical translation.